Atmospheric Environment 146 (2016) 79–89

Contents lists available at ScienceDirect

Atmospheric Environment

journal homepage: www.elsevier.com/locate/atmosenv

Spatial and seasonal variations of atmospheric sulfur concentrations and dry deposition at 16 rural and suburban sites in China

Xiaosheng Luo [a, b], Yuepeng Pan [c], Keith Goulding [d], Lin Zhang [e], Xuejun Liu [a, *], Fusuo Zhang [a]

[a] College of Resources and Environmental Sciences, Center for Resources, Environment and Food Security, Key Lab of Plant-Soil Interaction, MOE, China Agricultural University, Beijing, 100193, China
[b] Institute of Plant Nutrition, Resources and Environmental Sciences, Henan Academy of Agricultural Sciences, Henan Key Laboratory of Agricultural Eco-environment, Zhengzhou, 450002, China
[c] State Key Laboratory of Atmospheric Boundary Layer Physics and Atmospheric Chemistry (LAPC), Institute of Atmospheric Physics, Chinese Academy of Sciences, Beijing 100029, China
[d] The Sustainable Soils and Grassland Systems Department, Rothamsted Research, Harpenden, AL5 2JQ, UK
[e] Laboratory for Climate and Ocean-Atmosphere Studies, Department of Atmospheric and Oceanic Sciences, School of Physics, Peking University, Beijing, 100871, China

HIGHLIGHTS

- Sulfur (S) dry deposition was quantified at eight southern and eight northern sites in China.
- Total SO_2 plus pSO_4^{2-} deposition (3.1–27.1 kg S ha^{-1} yr^{-1}) showed large spatial variation across all sites.
- Concentration and dry deposition of S were remarkably higher at northern than southern sites.
- Low pSO_4^{2-}/pNO_3^- ratios at most sites reflected increasing NO_x relative to SO_2 emissions.

ARTICLE INFO

Article history:
Received 11 January 2016
Received in revised form
8 July 2016
Accepted 12 July 2016
Available online 14 July 2016

Keywords:
Acid rain
Particulate matter
SO_2
Sulfate
Dry deposition
China

ABSTRACT

The large emissions of sulfur dioxide (SO_2) in China have raised worldwide concerns due to its contribution to acid rain and particulate pollution. Monitoring sulfur (S) concentrations and estimating its deposition are important for evaluating air quality and its effects on ecosystems and human health. To date atmospheric dry S deposition in China remains unclear due to the paucity of measurements, especially in rural regions where the ecosystems are sensitive to acid deposition. In this study, we monitored both SO_2 and particulate SO_4^{2-} (pSO_4^{2-}) concentrations at 8 sites south and 8 sites north of the Huai River in rural and suburban parts of China between 2010 and 2012. The measured concentration of SO_2 and pSO_4^{2-} were combined with GEOS-Chem modeled dry deposition velocities to estimate dry S deposition inputs to the surfaces. SO_2 and pSO_4^{2-} concentrations were high from October/November to next March/April and they (esp. SO_2) decreased sharply since March/April at the northern sites, reflecting elevated SO_2 emissions by winter heating (which normally starts in October/November and ends in March/April in the north of the Huai River). However the southern sites did not show this trend. Annual dry deposition of SO_2 plus pSO_4^{2-} in this study ranged from 3.1 to 27.1 kg S ha^{-1} across all the sites in the year 2011 (except one site from May 2011 to April 2012) and showed large spatial variation. The sites in northern China had greater dry deposition due to the higher S concentrations compared with sites in southern China. We also found relatively low pSO_4^{2-}/pNO_3^- ratios at most sites, reflecting NO_x emissions had a larger influence than SO_2 emissions on particle composition during the 2010–2012 period at the measurement sites. Our results suggest that dry S deposition is still important input to ecosystems in spite of slow reduction of Chinese national SO_2 emissions since 2005. More research on both wet and dry S deposition and their impacts on the environment and human health should be carried out following the introduction of policies to reduce SO_2 emissions.

* Corresponding author.
E-mail address: liu310@cau.edu.cn (X. Liu).

http://dx.doi.org/10.1016/j.atmosenv.2016.07.038

1. Introduction

Global anthropogenic sulfur dioxide (SO_2) emissions increased rapidly from the 1850s and peaked in the 1970s (Smith et al., 2011), mainly caused by an increasing use of coal for industrial activities. As the precursor of sulfuric acid (H_2SO_4), gaseous SO_2 contributes to acid deposition, which affects the environment in a variety of ways (Su et al., 2011). H_2SO_4 can react with NH_3 to form NH_4HSO_4 and $(NH_4)_2SO_4$ in air (Fagerli and Aas, 2008), which contribute significantly to secondary aerosols with significant health and climate concerns (Mensah et al., 2012; Zhang et al., 2012a). Besides, SO_2 has many detrimental effects on the global environment such as soil and water acidification and direct damage to crop plants. In addition, sulfur (S) deposition can increase the emissions of nitrous oxide (N_2O) and nitric oxide (NO) from soil indirectly by acidifying the soil and increasing the proportions of these gases produced by denitrification, which has an adverse effect on global climate (Cai et al., 2012). In light of these concerns, control of SO_2 emission is crucial to improving air quality and decreasing damage to the environment and health worldwide. In fact, total global SO_2 emissions have decreased over the last 30 years, mainly due to substantial reductions in major developed economies such as North America and Europe as coal has been replaced by natural gas and other forms of energy (Sickles and Shadwick, 2015; Fowler et al., 2009).

Anthropogenic SO_2 emissions in China are an environmental concern because they have contributed approximately 25% of global emissions and more than 90% of those in East Asia since the 1990s (Lu et al., 2010). The very high SO_2 emissions in China are mainly due to both rapid economic development and the large consumption of coal. China's energy consumption structure lays particular stress on coal. The consumption of coal contributes to about 70% of total energy use - much more than the world average; 90% of national SO_2 emissions derive from coal burning (Kanada et al., 2013). The Chinese Government took measures to control SO_2 emissions following the 10th Five-Year Plan (2001–2005). However, the 10% reduction target from the 2000 level was not achieved by the end of 2005 (Lin et al., 2012). China therefore set new targets and effective measures to control SO_2 emissions, such as insisting that all new thermal power units as well as most existing units must have flue gas desulphurization (FGD) systems installed, and small units with low energy efficiency should be gradually shutdown. As a result, total national SO_2 emissions decreased by 14.3% from 2005 to 2010 (Zhao et al., 2008; Wang et al., 2012) and very significant decreases in SO_2 emissions and concentrations were reported in some Chinese megacities such as Beijing (SO_2 concentrations declined from 120 $\mu g\ m^{-3}$ in 1998 to 47 $\mu g\ m^{-3}$ in 2007) and Shanghai (SO_2 concentrations decreased by about 50% from 2005 to 2010) (Zhang et al., 2011; Wang et al., 2014). However, controlling SO_2 emissions still remains a big challenge for China because the economy and industry continue to develop, and some industrial facilities (such as iron, steel and cement works) continue to consume very large amounts of coal without installing desulfurization systems (Zhang et al., 2012b).

Sulfur deposited from emitted SO_2 has been regarded as the main contributor to acid deposition, which is an important environmental problem in China (Pan et al., 2013). Compared to developed countries, which conducted much research on S deposition, developing countries including China have conducted very little research (Fowler et al., 2009). Though China is the largest SO_2 emitter in the world, research into S deposition, especially dry deposition, is still lacking (Pan et al., 2013).

To determine the distribution of acid rain in China, many acid rain monitoring sites and programs have been introduced since the 1980s (Wang and Hao, 2012; Wang et al., 2012). However, the current national particulate sulfate (pSO_4^{2-}) monitoring network is poor, especially in rural regions, and cannot provide a complete analysis of SO_2 mitigation policy, in particular how it affects current particulate pollution and S deposition in China (Xin et al., 2015). China is a large agricultural country and the rural regions are very important for food production. As well as being a pollutant in natural ecosystems, S is one of the essential elements for plant growth and S deposition is an important input to croplands (Zhang et al., 2003). Therefore monitoring atmospheric S concentrations and calculating its dry deposition in typical Chinese rural regions will provide detailed information on the nutritional requirements of crops for S, the country's S pollution status, and the effectiveness of the SO_2 emission control measures.

In this study we selected 16 representative rural and suburban sampling sites, of which eight sites were located north of the Huai River (a border line dividing China into North and South in terms of its centralized home heating policy, with heating in the north but not the south), and eight sites were located south of the Huai river (shown in Fig. 1). We measured SO_2 and pSO_4^{2-} concentrations and calculated their dry deposition at the sampling sites. The objective of this study was to provide an overall evaluation of atmospheric S pollution and dry deposition, as well as their potential environmental effects in typical rural and suburban regions of China.

2. Materials and methods

2.1. Monitoring approach on SO_2 and pSO_4^{2-}

Atmospheric SO_2 and particulate sulfate (pSO_4^{2-}) were collected using a DELTA (DEnuder for Long-Term Atmospheric Sampling) system. The DELTA system contains denuders collecting reactive nitrogen (N) gases and SO_2 and filters to collect, in order, the particulate nitrate (pNO_3^-), particulate ammonium (pNH_4^+) and pSO_4^{2-}. The system contains a mini pump (air flow rate was 0.3 L min^{-1}) to maintain air flow though the denuders and filters (Tang et al., 2009). We used the system previously to monitor the atmospheric reactive N concentrations and estimate N deposition in different regions of China (Luo et al., 2013, 2014; Xu et al., 2015). The sampling frequency of the DELTA system was once per month at all the sampling sites. The first and second denuders were extracted with 10 ml 0.05% H_2O_2 solution. Following analysis of NO_3^--N and NH_4^+-N in the solution with a continuous-flow analyzer (Seal AA3, Germany), SO_4^{2-} (transformed from SO_2) in solution was measured by ion chromatography (761 Compact, Swiss); all analyses were made within one month of extraction. All the samples were refrigerated (at 4 °C) and the analyses made at China Agricultural University, Beijing. The sampling period was from the beginning to the end of each calendar month. After extraction and analysis, the concentration of S in air can be calculated from the measured concentrations and the volume of air passing through the Delta sampler. The formula for this is:

$$\chi_a = (C_e\text{-}C_b) \times \nu/V$$

where χ_a represents S concentration ($\mu g\ S\ m^{-3}$), C_e represents the concentration of S in the extract ($\mu g\ S\ L^{-1}$), C_b represents the concentration of S in the blank ($\mu g\ S\ L^{-1}$), ν represents the volume of the extract (L), and V the volume of air passing through the sampler during the sampling period (m^3). The sampling and S measurements were conducted at ambient temperature and air pressure and the final S concentrations and dry deposition fluxes at all sites were also expressed at ambient temperature and pressure.

2.2. Sampling sites and sampling period

A total of 16 sampling sites were established to monitor the SO_2

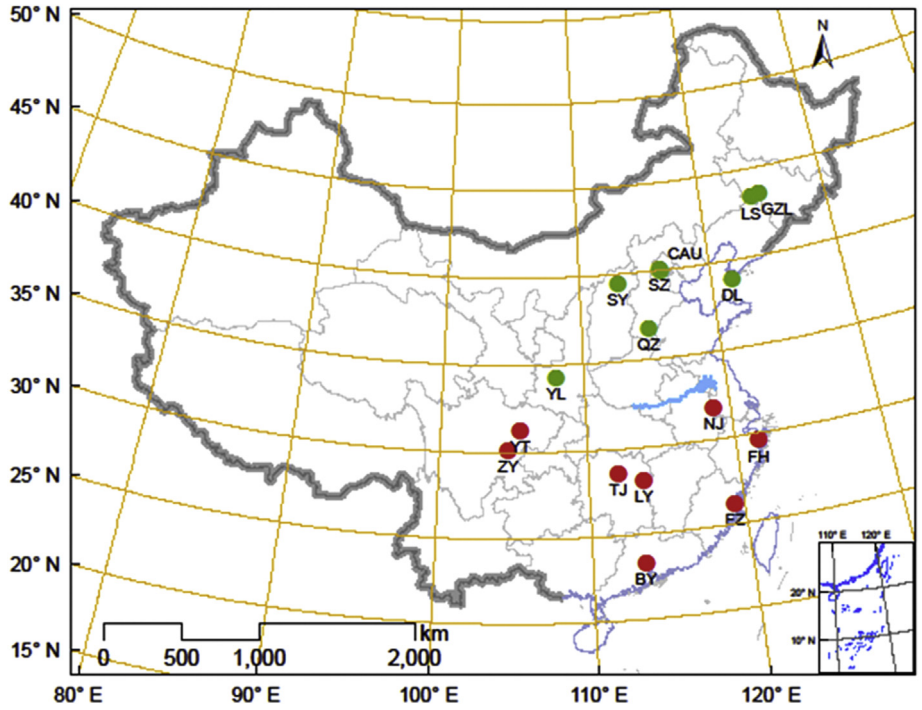

Fig. 1. Distribution of the sixteen sampling sites. Eight sampling sites north of the Huai River (Green circles) and eight were south of the Huai River (Red circles). Blue line represents the Huai River, Red color circles all belong to south China and green color circles belong to North China. (For interpretation of the references to color in this figure legend, the reader is referred to the web version of this article.)

and pSO_4^{2-} concentrations. All the sites were located in rural regions or suburban areas. Considering the observed close relationship between winter heating (coal burning induced SO_2 emissions) and SO_2 concentrations in air, we divided the monitoring sites into two groups: 8 sampling sites to the north of the Huai River (where heating is used in winter) and 8 sampling sites to the south of the Huai River (where there is no heating in winter). The distribution of specific sampling sites is shown in Fig. 1. The northern sampling sites were Lishu (LS), Gongzhuling (GZL), Dalian (DL), China Agricultural University (CAU), Shangzhuang (SZ), Quzhou (QZ), Yangling (YL) and Shanyin (SY). LS and GZL are in Jilin province and DL is in Liaoning province. All these three sampling sites can be regarded as being in the Northeast region of China. LS and GZL are rural, near farmland, where the crop was spring maize. DL is in a suburb of Dalian city, and is therefore a suburban site. The North China region contained 3 sampling sites which were CAU, SZ, and QZ. CAU and SZ are located in a suburb of Beijing, with CAU being closest to downtown Beijing. CAU and SZ belong to the experimental station of China Agricultural University and the crops grown during sampling were mainly winter wheat and summer maize. QZ was a rural site in Quzhou county, Hebei province, and the cropping system was a rotation of winter wheat and summer maize. YL is a rural site in Shaanxi province and the crops grown were also winter wheat and summer maize. SY was a rural site in north Shanxi province and the crop grown was mainly spring maize. The Southern sampling sites were Ziyang (ZY), Yanting (YT), Liuyang (LY), Taojiang (TJ), Nanjing (NJ), Fenghua (FH), Fuzhou (FZ), and Baiyun (BY). ZY and YT are in a rural region of Sichuan province and crops grown were wheat, rice and oilseed rape. LY and TJ are in Hunan province. LY is in a suburb of Changsha city and TJ is a rural site of Taojiang county. Double rice is the main cropping system at the two sites. NJ is a suburban site in Jiangsu province, and it is located at an experiment station of Nanjing Agricultural University and the crops grown were rice and wheat. FH is a rural site in Zhejiang province where the crops are mainly rice and vegetables. FZ is a mountainous rural site near Fuzhou city, Fujian province, where rice and tobacco are the main crops. BY is located at an Agricultural Experimental Station in a suburb of Guangzhou city, Guangdong province, and the cropping system is double rice. The monitoring started in 2010 and ended in 2012 at all sites except YT (monitoring started in 2011 and ended in 2012). Detailed sampling periods at all sites were as follows: QZ, SY (2010.4–2012.6), CAU, FZ, LS, SZ, YL (2010.4–2012.8), BY (2010.5–2012.8), ZY (2010.7–2012.2), GZL (2010.7–2012.8), FH (2010.8–2012.5), LY (2010.9–2012.2), NJ (2010.9–2012.6), DL (2010.9–2012.7), TJ (2010.10–2012.8), and YT (2011.5–2012.8).

2.3. Backward trajectories of SO_2 using TrajStat analysis

In order to identify the origin of air mass and the source of SO_2 from northern China, three-day backward trajectories arriving at five selected sampling sites (NJ, YT, TJ, FH, BY) during January, April, July and October in the monitoring period were calculated using TrajStat (version 1.4.4R4). TrajStat is a GIS-based software, including a trajectory calculation module of HYSPLIT (Hybrid Single Particle Lagrangian Integrated Trajectory Model) (Wang et al., 2009). Meteorological data with a resolution of $0.5^\circ \times 0.5^\circ$ were inputted from the Global Data Assimilation System (GDAS) meteorological data archives of the Air Resources Laboratory, National Oceanic and Atmospheric Administration (NOAA). All backward trajectories were calculated at 6 h intervals (00:00, 06:00, 12:00, 18:00 UTC) at each day, with an arrival height of 500 m above the ground.

2.4. Sulfur dry deposition

The inferential technique, which combines the measured concentration and a modeled dry deposition velocity (V_d), was used to estimate the dry deposition flux of S species (Schwede et al., 2011; Pan et al., 2012). The concentrations of gaseous SO_2 and pSO_4^{2-} were measured as described in Section 2.1. The V_d of SO_2 and pSO_4^{2-} were

calculated based on a GEOS-Chem chemical transport model (CTM) for all the sampling sites. In brief, the GEOS-Chem 3-D global CTM (http://geos-chem.org) was driven by GEOS-5 (Goddard Earth Observing System) assimilated meteorological data from the NASA Global Modeling and Assimilation Office (GMAO), with a temporal resolution of 6 h (3 h for surface variables and mixing depths) and a horizontal resolution of 1/2° latitude × 2/3° longitude. We used a nested-grid version of GEOS-Chem for Asia that has the native 1/2° × 2/3° resolution over East Asia (70°E–150°E, 11°S–55°N), and a 2° × 2.5° resolution over the rest of the world (Chen et al., 2009; Zhao et al., 2015). A similar nested model for North America has been previously applied to analyze N deposition over the United States (Zhang et al., 2012c; Ellis et al., 2013).

In GEOS-Chem parameterization of the dry deposition of gases and aerosols follows a standard big-leaf resistance-in-series model (Wesely, 1989). The V_d is calculated as the function $v_d = (R_a + R_b + R_c)^1$ determined by local meteorological conditions and surface type, as described in Zhang et al. (2012c). Here R_a is the aerodynamic resistance to turbulent transfer from the lowest model layer (70 m above the surface) to the roughness height, R_b is the boundary layer resistance to molecular diffusion, and R_c is the canopy or surface uptake resistance. In this study we have run the model calculation of dry deposition velocities for the whole of 2012 and archived the hourly values for both gases and aerosols over the model domain. Monthly V_d was then calculated based on the hourly outputs (Table 1) for further estimation of the dry deposition flux of each species during the observation period from 2010 to 2012.

Considerable uncertainties may exist due to the relatively coarse model 1/2° × 2/3° resolution for representing the local land characteristics at the monitoring sites. For the 16 sites, rural or cropland sites have relatively homogenous agricultural land uses within the model grid cell, while the land uses for suburban sites can be a mixture of croplands and some urban constructions. Further increasing the grid resolution for the V_d calculation would require assimilated meteorological fields at a finer resolution or in-situ meteorological measurements, which are not available at present. We compare the GEOS-5 derived V_d values with those from GEOS-FP data (a newer version replacing GEOS-5 with a finer resolution of 1/4° × 5/16°, yet only available after 2013). The hourly V_d values for SO_2 and pSO_4^{2-} can differ by 40%, but much smaller (15%) when averaged monthly.

We calculate the dry deposition fluxes for SO_2 and pSO_4^{2-} using the measured monthly mean concentrations multiplied by the modeled monthly V_d. It shall be acknowledged that this approach would omit the deposition covariance term associated with higher temporal variations, such as hourly and daily. In a study at a northeastern US forest site, Horii et al. (2005) found that the diel concentration and inferred deposition velocity of SO_2 had been shown to correlate strongly, with highest values in the daytime; thus, when average weekly SO_2 concentration was used to calculate the flux, $F(SO_2)$ can be systematically underestimated by as much as 40% (Matt and Meyers, 1993). Adon et al. (2013) suggested that this missing covariance term would induce an uncertainty of ~20% to dry deposition estimates of species with strong diurnal variations.

3. Results

3.1. Atmospheric SO_2 concentrations

Fig. 2 shows the monthly SO_2 concentrations at all 16 sampling sites. To show the results clearly, each sub-figure contains results from 4 sampling sites: Fig. 2 a and b represent the Northern region

Table 1
Monthly V_d (cm s^{-1}) of SO_2 and pSO_4^{2-} at the different sampling sites.

Site	Jan	Feb	Mar	Apr	May	Jun	Jul	Aug	Sep	Oct	Nov	Dec	Ave.
SO_2													
LS	0.30	0.30	0.30	0.32	0.37	0.48	0.54	0.52	0.47	0.36	0.26	0.20	0.37
GZL	0.30	0.29	0.30	0.30	0.36	0.50	0.54	0.52	0.48	0.34	0.26	0.20	0.37
DL	0.49	0.56	0.87	1.18	0.96	1.22	1.16	0.92	1.11	1.21	1.33	0.68	0.97
CAU	0.30	0.30	0.32	0.38	0.54	0.59	0.57	0.58	0.56	0.49	0.32	0.30	0.44
SZ	0.30	0.30	0.32	0.38	0.54	0.59	0.57	0.58	0.56	0.49	0.32	0.30	0.44
QZ	0.30	0.31	0.35	0.40	0.38	0.34	0.42	0.46	0.44	0.36	0.31	0.30	0.36
YL	0.29	0.30	0.34	0.42	0.48	0.48	0.47	0.50	0.48	0.40	0.31	0.30	0.40
SY	0.30	0.30	0.30	0.31	0.37	0.41	0.42	0.42	0.40	0.36	0.30	0.30	0.35
ZY	0.30	0.30	0.34	0.32	0.31	0.36	0.43	0.39	0.36	0.32	0.30	0.31	0.34
YT	0.31	0.33	0.36	0.36	0.38	0.42	0.45	0.44	0.43	0.39	0.34	0.31	0.38
LY	0.32	0.30	0.34	0.37	0.44	0.43	0.43	0.44	0.46	0.46	0.39	0.31	0.39
TJ	0.31	0.30	0.32	0.36	0.39	0.39	0.41	0.43	0.45	0.41	0.35	0.31	0.37
NJ	0.31	0.32	0.35	0.41	0.40	0.39	0.42	0.42	0.43	0.36	0.31	0.31	0.37
FH	0.31	0.32	0.35	0.41	0.45	0.42	0.43	0.48	0.47	0.40	0.34	0.30	0.39
FZ	0.67	0.69	0.71	0.70	0.71	0.76	0.72	0.74	0.68	0.69	0.65	0.65	0.70
BY	0.35	0.35	0.35	0.36	0.36	0.37	0.37	0.37	0.38	0.41	0.42	0.36	0.37
pSO_4^{2-}													
LS	0.10	0.13	0.15	0.20	0.25	0.19	0.21	0.19	0.17	0.13	0.09	0.07	0.15
GZL	0.10	0.13	0.16	0.20	0.25	0.19	0.19	0.19	0.16	0.13	0.09	0.07	0.16
DL	0.11	0.09	0.08	0.08	0.08	0.09	0.09	0.08	0.09	0.09	0.11	0.12	0.09
CAU	0.14	0.18	0.21	0.24	0.30	0.28	0.24	0.18	0.22	0.18	0.14	0.12	0.20
SZ	0.14	0.18	0.21	0.24	0.30	0.28	0.24	0.18	0.22	0.18	0.14	0.12	0.20
QZ	0.11	0.16	0.21	0.24	0.31	0.31	0.25	0.24	0.25	0.22	0.14	0.12	0.21
YL	0.14	0.17	0.19	0.24	0.27	0.32	0.23	0.24	0.20	0.19	0.15	0.12	0.21
SY	0.13	0.16	0.19	0.22	0.29	0.30	0.23	0.19	0.21	0.17	0.13	0.13	0.20
ZY	0.18	0.21	0.26	0.29	0.26	0.25	0.15	0.19	0.19	0.19	0.18	0.16	0.21
YT	0.16	0.18	0.21	0.26	0.25	0.26	0.14	0.18	0.17	0.17	0.16	0.14	0.19
LY	0.17	0.17	0.17	0.17	0.19	0.14	0.10	0.12	0.15	0.18	0.12	0.13	0.15
TJ	0.17	0.18	0.18	0.18	0.18	0.16	0.10	0.12	0.15	0.18	0.13	0.13	0.16
NJ	0.14	0.16	0.16	0.17	0.20	0.22	0.11	0.11	0.12	0.15	0.13	0.12	0.15
FH	0.15	0.16	0.17	0.17	0.16	0.12	0.09	0.12	0.12	0.14	0.13	0.12	0.14
FZ	0.11	0.12	0.14	0.12	0.13	0.11	0.09	0.10	0.11	0.11	0.10	0.10	0.11
BY	0.16	0.17	0.17	0.15	0.10	0.10	0.08	0.09	0.09	0.14	0.12	0.13	0.13

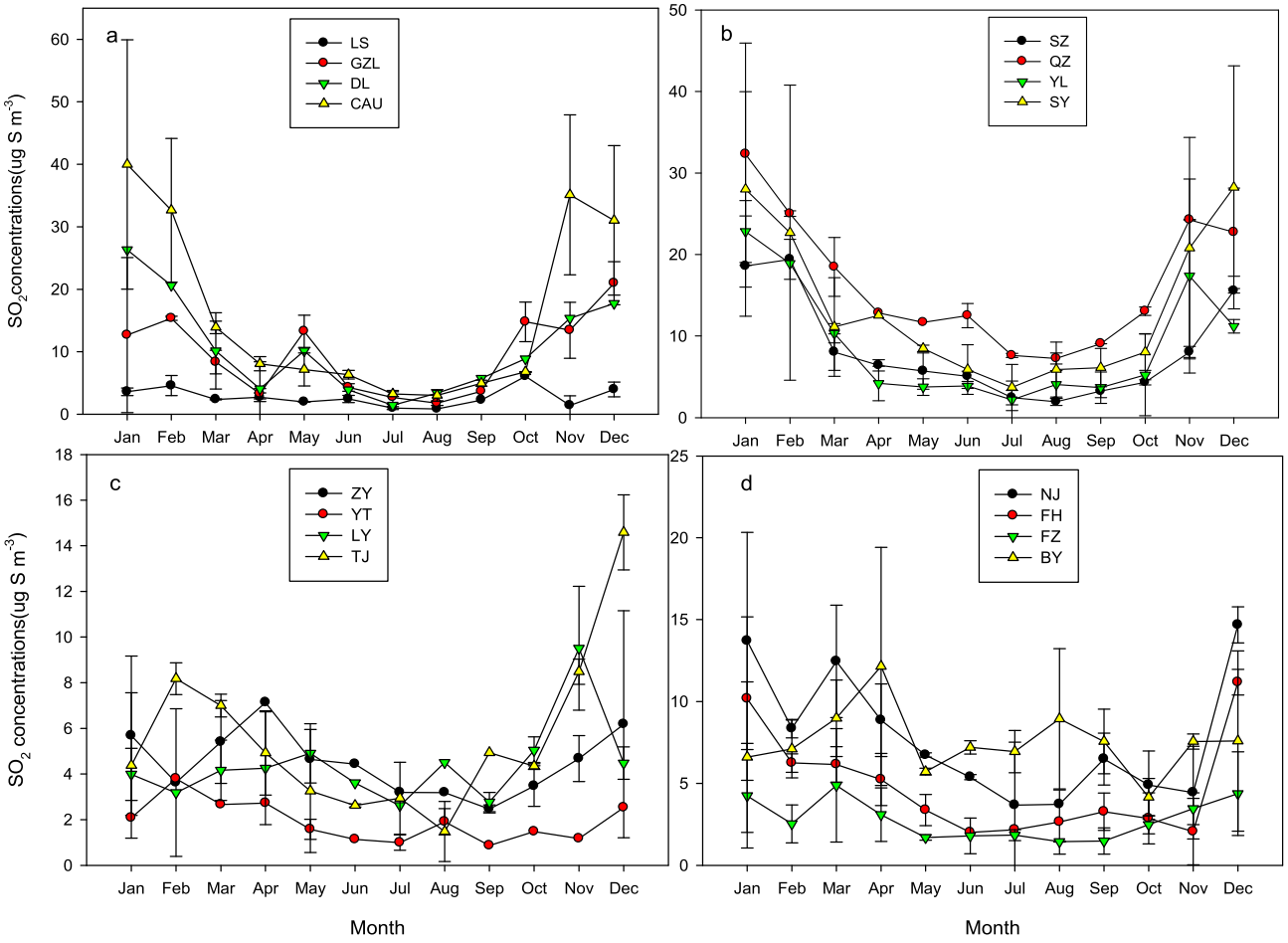

Fig. 2. Monthly average SO_2 concentrations at 16 sampling sites from varying monitoring period 2010 or 2011 to 2012 (μg S m^{-3}). a, b represent Northern China; c, d represent Southern China. Error bars represent the variations each month across the 1–3 years of sampling at each site, with warm season (April to August) monthly averages based on 2–3 years of data and cold season (September to March) on 1–2 years of data. The meaning of the ends of the whiskers represent minimum and maximum values of the monitoring period at each site.

(north of the Huai River) and Fig. 2 c and d the Southern region (south of the Huai River). Airborne SO_2 concentrations showed large seasonal variation in the North (Fig. 2a,b). Peak SO_2 concentrations mainly occurred in winter. LS and GZL are in the Northeast of China and the SO_2 concentrations there increased in October, consistent with the onset of winter heating provided by coal burning (usually starting in mid-October). SO_2 concentrations at the other sites DL, CAU, SZ, QZ, YL, SY increased sharply in November and also matched the onset of heating in these areas. Average SO_2 concentrations at LS, GZL, DL, CAU, SZ, QZ, YL, SY were 2.76 (27-month average), 9.54 (26-month average), 10.64 (23-month average), 16.01 (27-month average), 8.23 (27-month average), 16.40 (25-month average), 8.96 (27-month average), 13.46 (25-month average) μg S m^{-3}, respectively. The highest value was observed in QZ in Hebei province. The two sites in Beijing did not show very high SO_2 concentrations compared with other sites in Northern China.

Atmospheric SO_2 concentrations at Southern sites did not increase quite so obviously in the winter. Fig. 2c shows a peak SO_2 concentration in December at TJ but not at the other sites YT, LY, ZY. Fig. 2d indicates higher SO_2 concentrations (>10 μg S m^{-3}) at NJ and FH in December, January and March (March only for NJ) compared with other months, but with no strong peaks. The two southern tropical sites FZ and BY did not show any distinct seasonal variations of SO_2 concentrations (Fig. 2d). The average SO_2 concentrations at ZY, YT, LY, TJ, NJ, FH, FZ, BY were 4.51 (20-month average), 1.91 (16-month average), 4.42 (18-month average), 5.59 (23-month average), 7.78 (22-month average), 4.78 (22-month average), 2.77 (27-month average), 7.54 (28-month average) μg S m^{-3}, respectively. The sites with the highest average SO_2 concentrations were NJ and BY, two suburban sites. In general, SO_2 concentrations at southern sampling sites were lower than those at northern sites. Compared to the 8 southern sites, all the northern sites showed sharply decreased SO_2 concentrations after March, consistent with the time when heating stopped in northern China (Fig. 2).

In order to identify potential transport of SO_2 from the northern China, we calculated three-day backward trajectories arriving at five southern sites NJ, TY, TJ, FH, BY during January, April, July and October using the TrajStat. The TrajStat analysis showed that the transport of SO_2 from northern settlements would lead to an increase of SO_2 concentrations in winter south of Huai river, especially at the NJ site (Fig. 3). The high frequency of flow from north to south in the wintertime suggests that long range transport of SO_2 and perhaps pSO_4^{2-} from northern China could contribute to wintertime concentrations in the south.

3.2. *Atmospheric pSO_4^{2-} concentrations*

Monthly atmospheric pSO_4^{2-} concentrations at the sixteen sites are shown in Fig. 4. In contrast to SO_2 concentrations which peaked in winter at all northern sites, pSO_4^{2-} concentrations increased sharply in the winter only at CAU, QZ, and SY of the eight northern

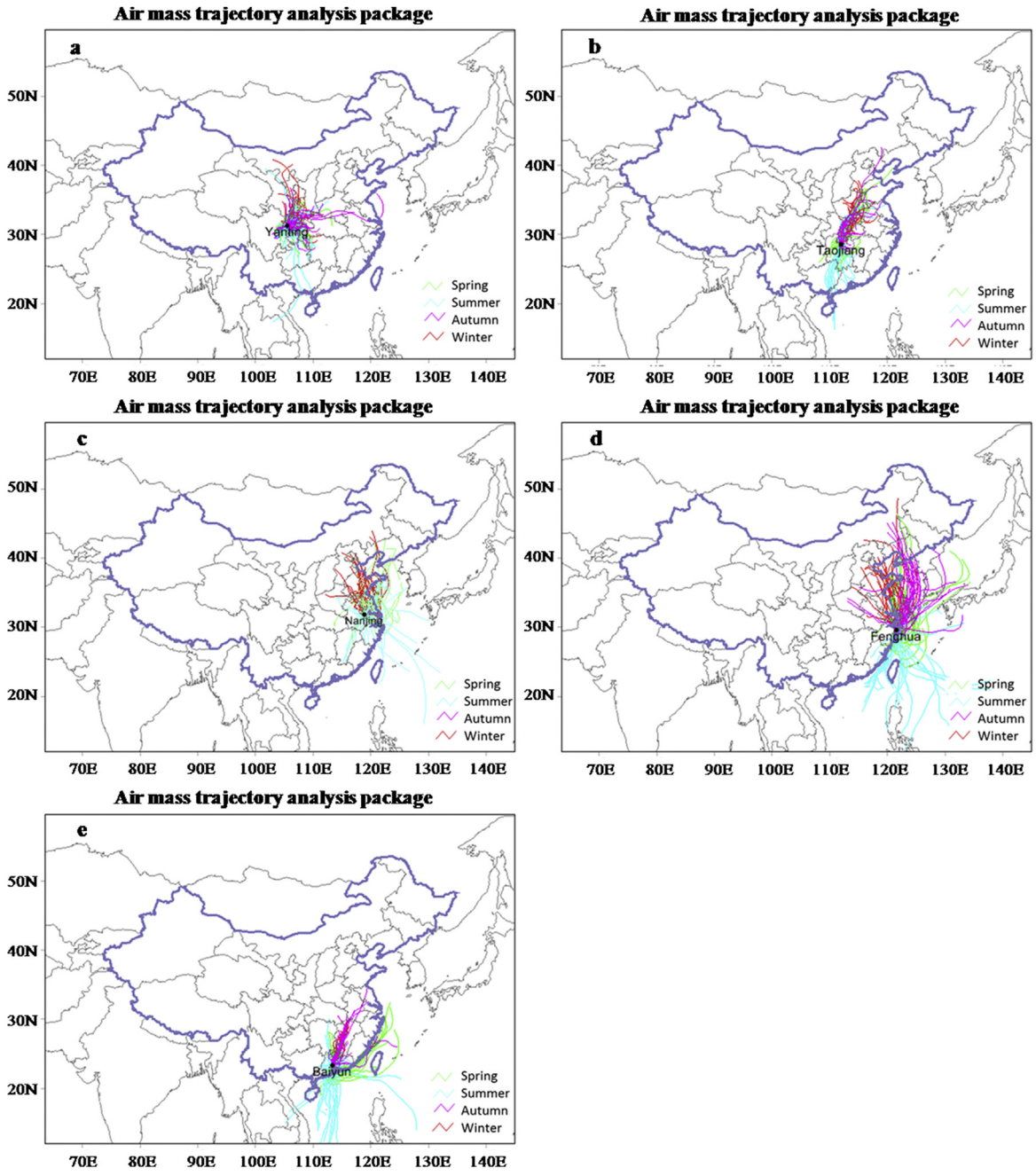

Fig. 3. HYSPLIT back-trajectories analysis on the path of air parcels (SO_2) prior to arrival at five selected sites in south China during different seasons (January-Winter, April-Spring, July-Summer, October-Autumn). "a, b, c, d, and e" represent Yanting (YT), Taojiang (TJ), Nanjing (NJ), Fenghua (FH), and Baiyun (BY) sites, respectively.

sites. Although GZL, DL, SZ, YL had higher SO_2 concentrations in winter, there were no obvious peak pSO_4^{2-} concentrations. The average pSO_4^{2-} concentrations were 1.00 (27-month average), 1.69 (26-month average), 1.40 (23-month average), 4.02 (27-month average), 2.51 (27-month average), 6.01 (25-month average), 2.05 (27-month average), 3.60 (25-month average) μg S m^{-3} at LS, GZL, DL, CA, SZ, QZ, YL, SY, respectively. The highest pSO_4^{2-} concentration was observed at QZ in Hebei province. This was consistent with the severe S (Pan et al., 2013) and reactive N pollution and deposition in the same area (Shen et al., 2009; Liu et al., 2013; Luo et al., 2013). The lowest pSO_4^{2-} concentrations were found at LS, a rural northeastern site. Seasonal pSO_4^{2-} concentrations did not show obvious variation at the southern sites. The average pSO_4^{2-} concentrations were 2.89 (20-month average), 1.23 (16-month average), 2.07 (18-month average), 1.47 (23-month average), 1.91 (22-month average), 1.47 (22-month average), 1.24 (27-month average), 1.99 (28-month average) μg S m^{-3} at ZY, YT, LY, TJ, NJ, FH, FZ, BY, respectively. The pSO_4^{2-} concentrations exhibited less spatial variation at the southern sites during the sampling period and high concentrations almost always occurred at the same time as high SO_2 concentrations.

3.3. Particulate sulfate, nitrate and ammonium ions characteristics at the sampling sites

The concentrations of SO_2, pSO_4^{2-}, pNO_3^-, pNH_4^+, the pSO_4^{2-}/pNO_3^- ratios (ratios of mass concentration) and the $([NH_4^+]-[NO_3^-])/[SO_4^{2-}]$

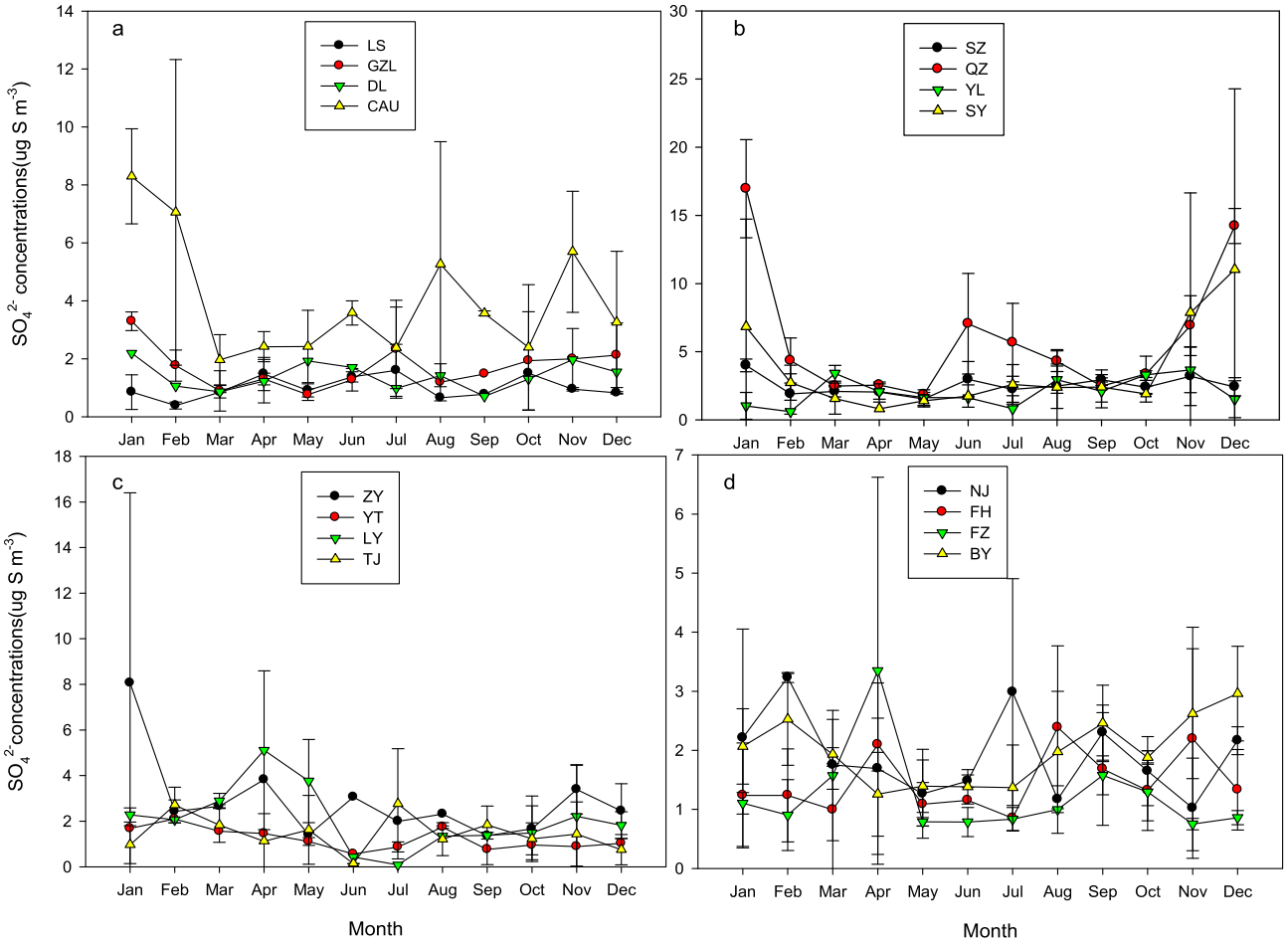

Fig. 4. Monthly average pSO_4^{2-} concentrations at 16 sampling sites during sampling period (μg S m^{-3}). a, b represent Northern China; c, d represent Southern China. Error bars represent the variations each month across the 1–3 years of sampling at each site, with warm season (April to August) monthly averages based on 2–3 years of data and cold season (September to March) on 1–2 years of data. The meaning of the ends of the whiskers represent minimum and maximum values of the monitoring period at each site.

ratios (ratios of micromolar concentrations), i.e. ($[NH_4^+]$-$[NO_3^-]$)/$[SO_4^{2-}]$ values (which were used to identify the NH_3-poor, -neutral, or -rich conditions) at all sampling sites are summarized in Table 2. The sum of major secondary aerosols pSO_4^{2-}, pNO_3^- and pNH_4^+ (SNA) concentrations ranged from 11.6 to 51.8 μg m^{-3} compared with SO_2 concentrations 3.65–33.2 μg m^{-3} (Table 2). Higher SNA concentrations appeared at the northern sites where severe particulate pollution existed (Pan et al., 2012); pNO_3^- was highest compared with that of pSO_4^{2-} and pNH_4^+ at the most sampling sites. The pSO_4^{2-}/pNO_3^- ratios were <1.0 at most sampling sites and reflected the increasing or stabilized NO_x emissions relative to reduced SO_2 emissions in many regions of China. H_2SO_4 and nitric acid (formed directly from SO_2 and NO_x, respectively) react with the NH_3 to form ammonium sulfate and ammonium nitrate in air, and H_2SO_4 react with NH_3 firstly. DSN values <2, = 2, and >2 indicate NH_3-poor (sulfate is insufficiently neutralized), NH_3-neutral (sulfate is exactly neutralized) and NH_3-rich (sulfate is sufficiently neutralized) condition (Wang et al., 2011; Dong et al., 2014), respectively. The average monthly DSN values were >2 at most sites in our monitoring period, suggesting that there was enough NH_3 to form nitrate particulates in the most months (Table 2). The average monthly DSN values of <2 at FZ and BY reflected NH_3 restricted conditions in the most months. Meanwhile, we found substantial variations for DSN for all sites, suggesting large seasonal and month-to-month variations of DSN in both north and south China. pNO_3^- and pNH_4^+ had significantly positive relationship across all sampling sites ($R^2 = 0.59$, $P < 0.01$). pSO_4^{2-} also correlated with pNH_4^+, although the correlation coefficient ($R^2 = 0.36$, $P < 0.05$) was lower than that between pNO_3^- and pNH_4^+.

3.4. Sulfur dry deposition

Deposition velocities of SO_2 ranged from 0.20 to 1.33 cm s^{-1}, being highest in the summer; while monthly deposition velocities of pSO_4^{2-} ranged from 0.07 to 0.32 cm s^{-1} (Table 1). Table 3 shows the 2011 (except YT from May 2011 to April 2012) dry deposition fluxes of SO_2, pSO_4^{2-} and total S species at the 16 sites. Dry SO_2 deposition ranged from 2.3 to 26.5 kg S ha^{-1} yr^{-1} and showed a large spatial variation across all the sites. Dry pSO_4^{2-} deposition (0.5–3.4 kg S ha^{-1} yr^{-1}) was much lower than that of SO_2 and showed much less spatial variation between all sites. Total dry S deposition (sum of SO_2 and pSO_4^{2-}) ranged from 3.1 to 27.1 kg S ha^{-1} yr^{-1} with average values at northern sites > southern sites (14.7 *vs* 7.6 kg S ha^{-1} yr^{-1}, $P < 0.05$). The lowest dry S deposition was at YT in southwest Sichuan while the highest deposition was at DL in Liaoning, northeast China. Dry deposition depends on both concentrations and deposition velocities of SO_2 and pSO_4^{2-}, so the highest dry S deposition did not occur at CAU (15.1 kg S ha^{-1} yr^{-1}) and QZ (10.6 kg S ha^{-1} yr^{-1}) where the highest S concentrations were observed but the deposition velocities here were smaller. Although dry deposition of both SO_2 and pSO_4^{2-} was estimated in current study, we realize that uncertainties cannot

Table 2
Sulfur dioxide, particulate sulfate (pSO_4^{2-}), nitrate (pNO_3^-) and ammonium (pNH_4^+) concentrations (μg m^{-3}), pNO_3^-/pSO_4^{2-} ratios (based on mass concentration) and DSN[#] values (ratios based on (micro)molar concentration, identifying the NH_3-poor (<2), -neutral (=2), or -rich (>2) conditions) at the sampling sites at ambient temperature and pressure.

Site	Gas or ions concentrations (μg m^{-3})				Ratio	Value
	SO_2	pSO_4^{2-}	pNO_3^-	pNH_4^+	pSO_4^{2-}/pNO_3^-	DSN[#]
LS	5.43 ± 3.00	3.07 ± 1.48	7.46 ± 3.06	9.45 ± 6.59	0.41 ± 0.14	14.9 ± 16.3
GZL	19.6 ± 13.9	5.05 ± 2.94	9.06 ± 3.54	6.69 ± 4.36	0.69 ± 0.77	4.12 ± 2.38
DL	20.3 ± 14.9	4.31 ± 1.61	8.98 ± 6.45	5.22 ± 2.45	0.60 ± 0.34	3.41 ± 1.55
CAU	31.0 ± 30.2	12.3 ± 8.24	21.8 ± 9.06	11.0 ± 6.79	0.69 ± 0.96	2.29 ± 3.60
SZ	16.0 ± 12.5	7.44 ± 3.31	13.7 ± 4.90	8.15 ± 5.35	0.63 ± 0.48	3.37 ± 4.92
QZ	33.2 ± 17.8	18.0 ± 4.83	20.0 ± 13.0	13.8 ± 7.22	1.06 ± 0.72	3.25 ± 2.68
YL	16.7 ± 14.6	6.45 ± 3.73	15.9 ± 12.3	14.3 ± 8.38	0.49 ± 0.27	10.0 ± 10.0
SY	26.4 ± 22.1	10.9 ± 14.7	11.9 ± 6.83	5.31 ± 2.77	0.72 ± 0.44	2.03 ± 2.56
ZY	9.05 ± 4.47	8.94 ± 8.40	9.77 ± 5.24	7.33 ± 4.79	1.19 ± 1.85	4.44 ± 4.90
YT	3.65 ± 1.70	3.62 ± 1.39	4.09 ± 1.50	4.97 ± 4.34	1.14 ± 0.89	4.56 ± 2.92
LY	9.06 ± 4.49	6.88 ± 5.21	9.19 ± 6.14	6.64 ± 4.09	1.22 ± 1.52	3.98 ± 3.22
TJ	11.24 ± 7.49	4.42 ± 3.35	3.98 ± 2.70	4.00 ± 2.49	1.34 ± 1.45	5.27 ± 5.02
NJ	16.55 ± 8.26	6.23 ± 2.90	13.8 ± 5.03	6.56 ± 2.80	0.45 ± 0.27	3.09 ± 3.46
FH	10.05 ± 6.82	4.62 ± 2.52	9.45 ± 3.29	5.23 ± 2.38	0.56 ± 0.47	4.44 ± 4.57
FZ	5.55 ± 3.45	3.69 ± 3.09	4.96 ± 1.37	2.93 ± 1.60	0.75 ± 0.51	1.95 ± 1.91
BY	15.19 (6.35)	5.93 (2.27)	12.1 ± 3.95	5.28 ± 2.89	0.51 ± 0.20	1.32 ± 2.12

[#] DSN = (($[pNH_4^+]$-$[pNO_3^-]$)/$[pSO_4^{2-}]$), where $[pNH_4^+]$, $[pNO_3^-]$ and $[pSO_4^{2-}]$ denotes micromolar concentrations (μmol m^{-3}) of particulate ammonium, nitrate and sulfate, respectively.

Table 3
Annual dry deposition of SO_2, pSO_4^{2-} and total S species at the 16 Chinese sampling sites in 2011 (except YT from May 2011 to April 2012, unit: kg S ha^{-1} yr^{-1}). Ave. and sd denote regional average deposition and standard deviation, respectively.

North- site	SO_2	pSO_4^{2-}	Total	South- site	SO_2	pSO_4^{2-}	Total
LS	3.37	1.16	4.53	**YT**	4.57	1.8	6.37
GZL	9.33	0.73	10.1	**ZY**	2.29	0.82	3.11
DL	26.5	0.65	27.1	**LY**	5.56	1.75	7.31
CAU	13.9	1.24	15.1	**TJ**	6.78	0.58	7.36
SZ	8.99	1.6	10.6	**NJ**	10.2	1	11.2
QZ	18.5	3.4	21.9	**FH**	6.18	0.5	6.68
YL	9.87	1.32	11.2	**FZ**	7.51	0.72	8.23
SY	14.3	2.49	16.8	**BY**	10.1	0.73	10.8
Ave. ± sd	13.1 ± 7.0	1.6 ± 0.9	14.7 ± 7.2	**Ave. ± sd**	6.6 ± 2.7	1.0 ± 0.5	7.6 ± 2.6

completely avoided because of (1) only a same whole one-year data used and (2) still some improvement space for calculating V_d of SO_2 and pSO_4^{2-} using the GEOS-Chem 3-D global CTM in the future.

4. Discussion

4.1. Atmospheric S concentrations and other inorganic ions in particulate matter

Our results show that high SO_2 concentrations occurred in the winter in northern China from 2010 to 2012 consistent with additional wintertime emissions in the north from home heating by coal burning (Fig. 2). That large emissions of SO_2 and other pollutants in winter contributed significantly to air pollution in northern China was observed in previous studies (Duan et al., 2005; Chan and Yao, 2008; Huang et al., 2014; Song et al., 2015). Centralized heating with coal contributed only 6.93% of the national SO_2 emissions in China in 2007 and was small compared to the emissions from power plants (Su et al., 2011). However, heating clearly made an important contribution to ground SO_2 concentrations; previous research showed that it can reach 39% of the total (Hao et al., 2005). This is because the height of the emission source from home heating is relatively low while those of power and industry point sources are always high. China's North Huai River Policy, which states that large scale heating for homes is only provided to the north of the Huai River, has a close relationship with air quality and people's health. Chen et al. (2013a) reported that the North Huai River Policy greatly increased pollution from total suspended particulates (TSPs) and led to negative health effects for the 500 million residents in Northern China, with more than 2.5 billion life years lost or a reduction of 5.5 years of life expectancy per person. Therefore taking more effective measures to reduce the SO_2 emissions in the North Huai River region when home heating is used is very important for winter air quality and human health.

SO_2 is the important precursor of pSO_4^{2-}, and so it makes a significant contribution to current $PM_{2.5}$ and PM_{10} pollution in China (Yang et al., 2011; Zhang et al., 2012a). As shown in Table 2, pNO_3^- was the dominant particulate component at most sites of SNA, which reflected higher NO_x emissions promoted more pNO_3^- formation in air at most sampling sites during the sampling periods. Another important factor is that most of our sampling sites, being in rural regions, have fewer local stationary SO_2 emissions (i.e. power plants, industry, etc). NH_3 plays a major role in the formation of pSO_4^{2-} and pNO_3^- in air because NH_3 reacts with H_2SO_4 firstly then with HNO_3 (Zhang et al., 2012d). Therefore higher NH_3 emissions will stimulate the transformation of NO_x to pNO_3^- (Wang et al., 2011). Of course, we believe there are indeed sources of pSO_4 (e.g., $CaSO_4$, transformed from H_2SO_4 reacting with $CaCO_3$) other than p $(NH_4)_2SO_4$ at the monitoring sites especially at sites in northern China where calcareous arable soils are widely distributed.

The higher pNO_3^-/pSO_4^{2-} ratios at sites in or near in Beijing and Shanghai are consistent with other similar studies (e.g., Chen et al., 2013b; Huang et al., 2012). There was a significant positive correlation between the average SO_2 concentrations and pSO_4^{2-}

concentrations ($r = 0.597$; $p < 0.05$) (Fig. 5), indicating that high SO_2 concentrations will promote the formation of pSO_4^{2-} in the air.

We calculated the monthly DSN values at all sampling sites during the sampling periods. We noticed the uncertainties of the DSN values due to the sea-salt and soil dust containing $NaNO_3$ and/or $CaSO_4$. Sea salt is one of the sources of aerosol which may affect the constitution of aerosols especially in coastal area. Sea salt contribution to PM was up to 5 μg m^{-3} at an urban area of Germany (Beuck et al., 2011). Sea salt source SO_4^{2-} and/or NO_3^- will potentially decrease the real DSN values of our study and the further research about how sea salt affect the ion concentrations and DSN values should be carried out in the future study. Lee et al. (1999) confirmed that soil-derived calcium from arid regions is an important contributor to base cation deposition, but also suggested that agricultural activities are a major regional source of airborne calcium. Authors of both studies pointed to large uncertainties in quantifying the sources and deposition rates of base cations. Zhang et al. (2012c) reported poor correlations between pSO_4^{2-} and pCa^{2+} in urban areas, but relationship between pSO_4^{2-} and pCa^{2+} is significantly different from rural sites, especially at remote sites exhibiting relative stronger neutralization of acidic sulfate by Ca^{2+}. Most of our sampling sites were in rural or near the farmland, so parts of pSO_4^{2-} (e.g., in the form of $CaSO_4$, transformed from H_2SO_4 reacting with $CaCO_3$) may be derived from soil dust, due to widely distributed calcareous soils in north and northwest China. The dust source pSO_4^{2-} in the air will underestimate the DSN values as well, which should be considered carefully in the future study.

As for concerns on why pSO_4^{2-} concentrations did not show similar seasonal variations to SO_2 concentration at the northern monitoring sites, our hypothesis is that there may be a 'buffering' system to form pSO_4^{2-} in different seasons. In winter or cold season, reduced NH_3 emission will limit the formation of ammonium sulfate and/or ammonium bisulfate (the majority of pSO_4^{2-}) when SO_2 emissions are high; in summer or warm season, coexistence of reactive N (NH_3 and NO_x) may enhance the transformation of pSO_4^{2-} from SO_2 when its emissions are low. Shen et al. (2009) reported high concentrations and deposition of reactive N species in North China Plain. The interactions and/or co-deposition of S and N species could partly explain the different seasonal variations of SO_2 and pSO_4^{2-} (Shen et al., 2011; Wang et al., 2013).

China has achieved the SO_2 emission reduction targets in both the 11th Five-Year Plan (FYP) (2006–2010), and the 12th FYP (2011–2015). However, there was no target for NO_x emission reduction in the 11th FYP (2006–2010), and only a small reduction target in the 12th FYP (2011–2015). If the NOx emissions increased in 12th FYP (2011–2015), nitrate will be the most important part of the three inorganic components (sulfate, nitrate and ammonium) in the secondary particulates in South and North China (Wang et al., 2013). Controlling SO_2 emissions will change the composition of secondary aerosols and/or particles. In the United States, modeling results showed that particulate matter would contain more pNO_3^- if SO_2 emissions decreased (Pye et al., 2009). However, China began to control SO_2 emissions only recently. How SO_2 emission control policy will affect China's air quality (e.g. SO_2 and $PM_{2.5}$) requires further research and long-term observation.

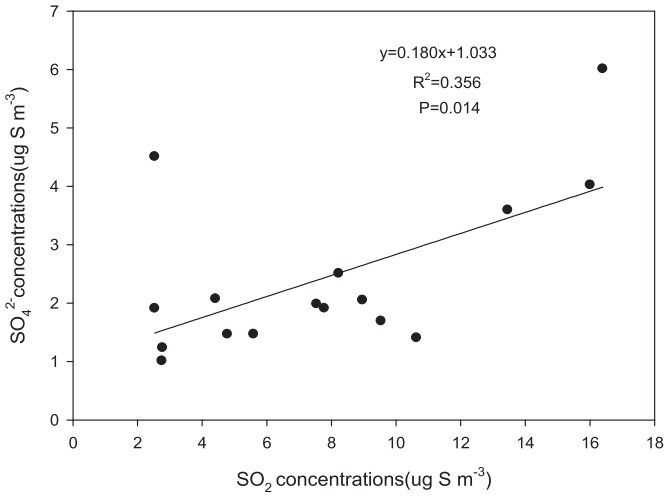

Fig. 5. Correlation between average SO_2 concentrations and pSO_4^{2-} concentrations across 16 monitoring sites.

4.2. Sulfur dry deposition and its implications

Acid rain is closely related to S deposition, but research into S deposition has mainly focused on wet deposition in China (Pan et al., 2013). Compared with north China, the south of China has a higher rainfall and more acidic soils (Guo et al., 2010) and its precipitation is more acidic. So the wet deposition of S has been studied much more intensively in southern China. Aas et al. (2007) surveyed SO_2 weekly concentrations at five sites in southern China in 2001–2003, where the annual average concentrations ranged from lower values of 0.55–2.59 μg S m^{-3} to the highest values of 37.2–42.7 μg S m^{-3}, showing large spatial variation. The precipitation-weighted mean concentration of SO_4^{2-} in rainwater ranged from 41.8 to 1227.6 μeq L^{-1} (every rain event) in Chengdu in 2008 (Wang and Han, 2011). Annual average wet deposition of SO_4^{2-}-S at two sites in southeastern China were 31.0 and 87.2 kg S ha^{-1} respectively during 2010 and 2011 (Cui et al., 2014). Pan et al. (2013) reported dry deposition of S at ten sites in northern China between December 2007 and November 2010, which ranged from 20.4 to 80.0 kg S ha^{-1} yr^{-1} with an average value of 45.2 kg S ha^{-1} yr^{-1}; the lowest value was at a rural site. In our study, dry deposition at the northern Chinese sites was 3.1–27.1 kg S ha^{-1} yr^{-1} in 2011 (Table 3), i.e. much smaller than values at urban sites but closer to the lowest rural site (20.4 kg S ha^{-1} yr^{-1}) recorded by Pan et al. (2013). The monthly V_d of SO_2 were 0.30–0.59 cm s^{-1} in northern China of our study (5 sampling sites: CAU, SZ, QZ, YL, SY). Pan et al. (2013) had similar V_d values (0.15–0.77 cm s^{-1}) to estimate S dry deposition in northern China. So the lower concentrations of SO_2 and pSO_4^{2-} at our monitoring sites than the sites in Pan et al. (2013) should explain the relatively low atmospheric dry S deposition in northern China. This may reflect the decreased SO_2 emissions with the Chinese emission control policy for SO_2.

5. Conclusion

Acid deposition is formed from a range of anthropogenic and natural emissions, including SO_2 and NO_x. These gases can be transformed to H_2SO_4 and HNO_3in the atmosphere and which can form condensation nuclei for aerosols and clouds, acidifying precipitation. Since S deposition has declined dramatically across Europe, N is now making a greater contribution to acid rain than S on a mass basis at current deposition levels. China has taken effective measures to control SO_2 emission since the 10th FYP (2001–2005) and, if this trend continues, S deposition will further decrease. As in Europe, this will have interesting and potentially important effects on ecosystems and human health in China that should be researched. The higher pNO_3^-/pSO_4^{2-} (mass basis) at most sampling sites reflected relative importance of mobile sources for the particulates formation in our study. We evaluated only the dry deposition of S, and only at 16 representative rural and suburban sampling sites. Monitoring the deposition of both dry and wet

forms is necessary for a more complete evaluation of S deposition and its effects. Also the present research was conducted before 2012. More work is needed under current conditions to keep pace with the SO_2 emission control policy of China. Taking more effective measures to reduce the SO_2 emissions here will be very important for winter air quality and human health.

Acknowledgements

This work was financially supported by Chinese National Basic Research Programme (2014CB954202, 2016YFD0800101 and 2012CB417100), China National Funds for Distinguished Young Scientists (40425007), and the National Natural Science Foundation of China (31421092, 41405144 and 41321064).

References

Aas, W., Shao, M., Jin, L., Larssen, T., Zhao, D.W., Xiang, R.J., Zhang, J.H., Xiao, J.S., Duan, L., 2007. Air concentrations and wet deposition of major inorganic ions at five non-urban sites in China, 2001–2003. Atmos. Environ. 41, 1706–1716.

Adon, M., Galy-Lacaux, C., Delon, C., Yoboue, V., Solmon, F., Kaptue Tchuente, A.T., 2013. Dry deposition of nitrogen compounds (NO2, HNO3, NH3), sulfur dioxide and ozone in west and central African ecosystems using the inferential method. Atmos. Chem. Phys. 13, 11351–11374.

Beuck, H., Quass, U., Klemm, O., Kuhlbusch, T.A.J., 2011. Assessment of sea salt and mineral dust contributions to PM10 in NW Germany using tracer models and positive matrix factorization. Atmos. Environ 45, 5813–5821.

Cai, Z.C., Zhang, J.B., Zhu, T.B., Cheng, Y., 2012. Stimulation of NO and N_2O emissions from soils by SO_2 deposition. Glob. Change Biol. 18, 2280–2291.

Chan, C.K., Yao, X.H., 2008. Air pollution in mega cities in China. Atmos. Environ. 42, 1–42.

Chen, Y.Y., Ebenstein, A., Greenstone, M., Li, H.B., 2013a. Evidence on the impact of sustained exposure to air pollution on life expectancy from China's Huai River policy. Proc. Natl. Acad. Sci. U. S. A. 110, 12936–12941.

Chen, S.Y., Lang, J.L., Zhou, Y., Han, L.H., Wang, G., Chen, D.S., 2013b. A new monitoring-simulation-source apportionment approach for investigating the vehicular emission contribution to the $PM_{2.5}$ pollution in Beijing, China. Atmos. Environ. 79, 308–316.

Chen, D., Wang, Y.X., McElroy, M.B., He, K., Yantosca, R.M., Le Sager, P., 2009. Regional CO pollution in China simulated by high-resolution nested-grid GEOS-Chem model. Atmos. Chem. Phys. 11, 3825–3839.

Cui, J., Zhou, J., Peng, Y., He, Y.Q., Yang, H., Mao, J.D., Zhang, M.L., Wang, Y.H., Wang, S.W., 2014. Atmospheric wet deposition of nitrogen and sulfur in the agroecosystem in developing and developed areas of Southeastern China. Atmos. Environ. 89, 102–108.

Duan, F.K., He, K.B., Ma, Y.L., Jia, Y.T., Yang, F.M., Lei, Y., Tanaka, S., Okuta, T., 2005. Characteristics of carbonaceous aerosols in Beijing, China. Chemosphere 60, 355–364.

Dong, X.Y., Li, J., Fu, J.S., Gao, Y., Huang, K., Zhuang, G.S., 2014. Inorganic aerosols responses to emission changes in Yangtze River Delta, China. Sci. Total Environ. 481, 522–532.

Ellis, R.A., Jacob, D.J., Sulprizio, M.P., Zhang, L., Holmes, C.D., Schichtel, B.A., Blett, T., Porter, E., Pardo, L.H., Lynch, J.A., 2013. Present and future nitrogen deposition to national parks in the United States: critical load exceedances. Atmos. Chem. Phys. 13, 9083–9095.

Fowler, D., Pilegaard, K., Sutton, M.A., Ambus, P., Raivonen, M., Duyzer, J., Simpson, D., Fagerli, H., Fuzzi, S., Schjoerring, J.K., Granier, C., Neftel, A., Isaksen, I.S.A., Laj, P., Maione, M., Monks, P.S., Burkhardt, J., Daemmgen, U., Neirynck, J., Personne, E., Wichink-Kruit, R., Butterbach-Bahl, K., Flechard, C., Tuovinen, J.P., Coyle, M., Gerosa, G., Loubet, B., Altimir, N., Gruenhage, L., Ammann, C., Cieslik, S., Paoletti, E., Mikkelsen, T.N., Ro-Poulsen, H., Cellier, P., Cape, J.N., Horváth, L., Loreto, F., Niinemets, Ü., Palmer, P.I., Rinne, J., Misztal, P., Nemitz, E., Nilsson, D., Pryor, S., Gallagher, M.W., Vesala, T., Skiba, U., Brüggemann, N., Zechmeister-Boltenstern, S., Williams, J., O'Dowd, C., Facchini, M.C., de Leeuw, G., Flossman, A., Chaumerliac, N., Erisman, J.W., 2009. Atmospheric composition change: ecosystems–atmosphere interactions. Atmos. Environ. 43, 5193–5267.

Fagerli, H., Aas, W., 2008. Trends of nitrogen in air and precipitation: model results and observations at EMEP sites in Europe, 1980-2003. Environ. Pollut. 154, 448–461.

Guo, J.H., Liu, X.J., Zhang, Y., Shen, J.L., Han, W.X., Zhang, W.F., Christie, P., Goulding, K., Vitousek, P., Zhang, F.S., 2010. Significant soil acidification in major Chinese croplands. Science 327, 1008–1010.

Hao, J., Wang, L., Li, L., Hu, J.N., Yu, X.C., 2005. Air pollutants contribution and control strategies of energy-use related sources in Beijing. Sci. China Ser. D 48 (Suppl. II), 138–146.

Horii, C.V., William Munger, J., Wofsy, S.C., Zahniser, M., Nelson, D., Barry McManus, J., 2005. Atmospheric reactive nitrogen concentration and flux budgets at a Northeastern U.S. forest site. Agric. For. Meteorol. 133, 210–225.

Huang, K., Zhuang, G., Lin, Y., Fu, J.S., Wang, Q., Liu, T., Zhang, R., Jiang, Y., Deng, C., Fu, Q., Hsu, N.C., Cao, B., 2012. Typical types and formation mechanisms of haze in an Eastern Asia megacity, Shanghai. Atmos. Chem. Phys. 12, 105–124.

Huang, R.J., Yanlin Zhang, Y.L., Bozzetti, C., Ho, K.F., Cao, J.J., Han, Y.M., Daellenbach, K.R., Slowik, J.G., Platt, S.M., Canonaco, F., Zotter, P., Wolf, R., Pieber, S.M., Bruns, E.A., Crippa, M., Ciarelli, G., Piazzalunga, A., Schwikowski, M., Abbaszade, G., Schnelle-Kreis, J., Zimmermann, R., An, Z.S., Szidat, S., Baltensperger, U., Haddad, I.E., Prévót, A.S.H., 2014. High secondary aerosol contribution to particulate pollution during haze events in China. Nature 514, 218–222.

Kanada, M., Dong, L., Fujita, T., Fujii, M., Inoue, T., Hirano, Y., Togawa, T., Geng, Y., 2013. Regional disparity and cost-effective SO_2 pollution control in China: a case study in 5 mega-cities. Energy Policy 61, 1322–1331.

Lee, D.S., Kingdon, R.D., Pacyna, J.M., Bouwman, A.F., Tegens, I., 1999. Modelling base cations in European sources, transport and deposition of calcium. Atmos. Environ 33, 2241–2256.

Lin, W.L., Xu, X.B., Ma, Z.Q., Zhao, H.R., Liu, X.W., Wang, Y., 2012. Characteristics and recent trends of sulfur dioxide at urban, rural, and background sites in North China: effectiveness of control measures. J. Environ. Sci. 24, 34–49.

Liu, X.J., Zhang, Y., Han, W.X., Tang, A.H., Shen, J.L., Cui, Z.L., Vitousek, P., Erisman, J.W., Goulding, K., Christie, P., Fangmeier, A., Zhang, F.S., 2013. Enhanced nitrogen deposition over China. Nature 494, 459–462.

Luo, X.S., Liu, P., Tang, A.H., Liu, J.Y., Zong, X.Y., Zhang, Q., Kou, C.L., Zhang, L.J., Fowler, D., Fangmeier, A., Christie, P., Zhang, F.S., Liu, X.J., 2013. An evaluation of atmospheric Nr pollution and deposition in North China after the Beijing Olympics. Atmos. Environ. 74, 209–216.

Luo, X.S., Tang, A.H., Shi, K., Wu, L.H., Li, W.Q., Shi, W.Q., Shi, X.K., Erisman, J.W., Zhang, F.S., Liu, X.J., 2014. Chinese coastal seas are facing heavy atmospheric nitrogen deposition. Environ. Res. Lett. 9, 095007.

Lu, Z., Streets, D.G., Zhang, Q., Wang, S., Carmichael, G.R., Cheng, Y.F., Wei, C., Chin, M., Diehl, T., Tan, Q., 2010. Sulfur dioxide emissions in China and sulfur trends in East Asia since 2000. Atmos. Chem. Phys. 10, 6311–6331.

Mensah, A.A., Holzinger, R., Otjes, R., Trimborn, A., Mentel, T.F., Brink, H. ten, Henzing, B., Kiendler-Scharr, A., 2012. Aerosol chemical composition at Cabauw, the Netherlands as observed in two intensive periods in May 2008 and March 2009. Atmos. Chem. Phys. 12, 4723–4742.

Matt, D.R., Meyers, T.P., 1993. On the use of the inferential technique to estimate dry deposition of SO_2. Atmos. Environ. 27A, 493–501.

Pan, Y.P., Wang, Y.S., Tang, G.Q., Wu, D., 2013. Spatial distribution and temporal variations of atmospheric sulfur deposition in Northern China: insights into the potential acidification risks. Atmos. Chem. Phys. 13, 1675–1688.

Pan, Y.P., Wang, Y.S., Tang, G.Q., Wu, D., 2012. Wet and dry deposition of atmospheric nitrogen at ten sites in Northern China. Atmos. Chem. Phys. 12, 6515–6535.

Pye, H.O.T., Liao, H., Wu, S., Mickley, L.J., Jacob, D.J., Henze, D.K., Seinfeld, J.H., 2009. Effect of changes in climate and emissions on future sulfate-nitrate-ammonium aerosol levels in the United States. J. Geophys. Res. 114, 1–18.

Schwede, D., Zhang, L., Vet, R., Lear, G., 2011. An intercomparison of the deposition models used in the CASTNET and CAPMoN networks. Atmos. Environ. 45, 1337–1346.

Shen, J.L., Tang, A.H., Liu, X.J., Fangmeier, A., Goulding, K.W.T., Zhang, F.S., 2009. High concentrations and dry deposition of reactive nitrogen species at two sites in the North China Plain. Environ. Pollut. 157, 3106–3113.

Shen, J.L., Liu, X.J., Zhang, Y., Fangmeier, A., Goulding, K., Zhang, F., 2011. Atmospheric ammonia and particulate ammonium from agricultural sources in the North China Plain. Atmos. Environ. 45, 5033–5041.

Sickles II, J.E., Shadwick, D.S., 2015. Air quality and atmospheric deposition in the eastern US: 20 years of change. Atmos. Chem. Phys. 15, 173–197.

Smith, S.J., van Aardenne, J., Klimont, Z., Andres, R.J., Volke, A., Delgado Arias, S., 2011. Anthropogenic sulfur dioxide emissions: 1850–2005. Atmos. Chem. Phys. 11, 1101–1116.

Song, W., Chang, Y.H., Liu, X.J., Li, K.H., Gong, Y.M., He, G.X., Wang, X.L., Christie, P., Zheng, M., Dore, A.J., Tian, C., 2015. A multiyear assessment of air quality benefits from China's emerging shale gas revolution: urumqi as a case study. Environ. Sci. Technol. 49, 2066–2072.

Su, S.S., Li, B.G., Cui, S.Y., Tao, S., 2011. Sulfur dioxide emissions from combustion in China: from 1990 to 2007. Environ. Sci. Technol. 45, 8403–8410.

Tang, Y.S., Simmons, I., Dijk, N.V., Marco, C.D., Nemitz, E., Dämmgen, U., Gilke, K., Djuricic, V., Vidic, S., Gliha, Z., Borovecki, D., Mitosinkova, M., Hanssen, J.E., Uggerud, T.H., Sanz, M.J., Sanz, P., Chorda, J.V., Flechard, C.R., Fauvel, Y., Ferm, M., Perrino, C., Sutton, M.A., 2009. European scale application of atmospheric reactive nitrogen measurements in a low-cost approach to infer dry deposition fluxes. Agric. Ecosyst. Environ. 133, 183–195.

Wang, H., Han, G.L., 2011. Chemical composition of rainwater and anthropogenic influences in Chengdu, Southwest China. Atmos. Res. 99, 190–196.

Wang, S.X., Xing, J., Jang, C., Zhu, Y., Fu, J.S., Hao, J.M., 2011. Impact assessment of ammonia emissions on inorganic aerosols in East China using response surface modeling technique. Environ. Sci. Technol. 45, 9293–9300.

Wang, Y., Yu, W., Pan, Y., Wu, D., 2012. Acid neutralization of precipitation in Northern China. J. Air Waste Manag. Assoc. 62, 204–211.

Wang, Y., Zhang, Q.Q., He, K., Zhang, Q., Chai, L., 2013. Sulfate-nitrate-ammonium aerosols over China: response to 2000–2015 emission changes of sulfur dioxide, nitrogen oxides, and ammonia. Atmos. Chem. Phys. 13, 2635–2652.

Wang, Y.Q., Zhang, X.Y., Draxler, R.R., 2009. TrajStat: GIS-based software that uses various trajectory statistical analysis methods to identify potential sources from long-term air pollution measurement data. Environ. Model. Softw. 24,

938–939.
Wang, S.X., Hao, J.M., 2012. Air quality management in China: issues, challenges, and options. J. Environ. Sci. 24, 2–13.
Wang, S.X., Xing, J., Zhao, B., Jang, C., Hao, J.M., 2014. Effectiveness of national air pollution control policies on the air quality in metropolitan areas of China. J. Environ. Sci. 26, 13–22.
Wesely, M.L., 1989. Parameterization of surface resistances to gaseous dry deposition in regional-scale numerical-models. Atmos. Environ. 23, 1293–1304.
Xin, J., Wang, Y., Pan, Y., Ji, D., Liu, Z., Wen, T., Wang, Y., Li, X., Sun, Y., Sun, J., Wang, P., Wang, G., Wang, X., Cong, Z., Song, T., Hu, B., Wang, L., Tang, G., Gao, W., Guo, Y., Miao, H., Tian, S., Wang, L., 2015. The campaign on atmospheric aerosol research network of China: CARE-China. Bull. Am. Meteorol. Soc. 96, 1137–1155.
Xu, W., Luo, X.S., Pan, Y.P., Zhang, L., Tang, A.H., Shen, J.L., Zhang, Y., Li, K.H., Wu, Q.H., Yang, D.W., Zhang, Y.Y., Xue, J., Li, W.Q., Li, Q.Q., Tang, L., Lu, S.H., Liang, T., Tong, Y.A., Liu, P., Zhang, Q., Xiong, Z.Q., Shi, X.J., Wu, L.H., Shi, W.Q., Tian, K., Zhong, X.H., Shi, K., Tang, Q.Y., Zhang, L.J., Huang, J.L., He, C.E., Kuang, F.H., Zhu, B., Liu, H., Jin, X., Xin, Y.J., Shi, X.K., Du, E.Z., Dore, A.J., Tang Jr., S., Collett, J.L., Goulding, K., Sun, Y.X., Ren, J., Zhang, F.S., Liu, X.J., 2015. Quantifying atmospheric nitrogen deposition in China through a nationwide monitoring network. Atmos. Chem. Phys. 15, 12345–12360.
Yang, F., Tan, J., Zhao, Q., Du, Z., He, K., Ma, Y., Duan, F., Chen, G., Zhao, Q., 2011. Characteristics of PM2.5 speciation in representative megacities and across China. Atmos. Chem. Phys. 11, 5207–5219.
Zhang, M., Wang, T.J., Zhang, Y., Hu, Z.Y., Xu, C.K., 2003. Observational study on atmospheric sulfur deposition to farmland ecosystem. Sci. Meteorol. Sin. 23, 263–272.
Zhang, J., Ouyang, Z.Y., Miao, H., Wang, X.K., 2011. Ambient air quality trends and driving factor analysis in Beijing, 1983–2007. J. Environ. Sci. 23, 2017–2018.
Zhang, X.Y., Wang, Y.Q., Niu, T., Zhang, X.C., Gong, S.L., Zhang, Y.M., Sun, J.Y., 2012a. Atmospheric aerosol compositions in China: spatial/temporal variability, chemical signature, regional haze distribution and comparisons with global aerosols. Atmos. Chem. Phys. 12, 779–799.
Zhang, Q., He, K.B., Huo, H., 2012b. Cleaning China's air. Nature 484, 161–162.
Zhang, L., Jacob, D.J., Knipping, E.M., Kumar, N., Munger, J.W., Carouge, C.C., van Donkelaar, A., Wang, Y.X., Chen, D., 2012c. Nitrogen deposition to the United States: distribution, sources, and processes. Atmos. Chem. Phys. 12, 4539–4554.
Zhang, X.Y., Jiang, H., Jin, J.X., Xu, X.H., Zhang, Q.X., 2012d. Analysis of acid rain patterns in northeastern China using a decision tree method. Atmos. Environ. 46, 590–596.
Zhao, Y., Wang, S.X., Duan, L., Lei, Y., Cao, P.F., Hao, J.M., 2008. Primary air pollutant emissions of coal-fired power plants in China: current status and future prediction. Atmos. Environ. 42, 8442–8452.
Zhao, Y., Zhang, L., Pan, Y., Wang, Y., Paulot, F., Henze, D.K., 2015. Atmospheric nitrogen deposition to the northwestern Pacific: seasonal variation and source attribution. Atmos. Chem. Phys. 15, 10905–10924.